Int j simul model 23 (2024) 4, 599-610
Original scientific paper

GA AND WOA-BASED OPTIMIZATION FOR ELECTRIC POWERTRAIN EFFICIENCY

Savran, E.[*]; Karpat, E.[**] & Karpat, F.[*]
[*] Mechanical Engineering Department, Bursa Uludag University, 16059, Bursa, Turkey
[**] Electrical-Electronics Engineering Department, Bursa Uludag University, 16059, Bursa, Turkey
E-Mail: efesavran@uludag.edu.tr, esinoz@uludag.edu.tr, karpat@uludag.edu.tr

Abstract
This study presents an optimum vehicle architecture along with a design methodology that optimizes the motor power, battery capacity, and propulsion ratio for two different driving profiles using Genetic Algorithm (GA) and Whale Optimization Algorithm (WOA). A virtual electric vehicle model was created in MATLAB/Simulink and validated with real-world driving. The vehicle architecture was optimized with GA and WOA based on the cost, range, gradability, and maximum speed outputs obtained from the "hybrid driving" and "urban driving" behaviours. According to the results obtained in the study, it was found that GA optimization can create a vehicle architecture suitable for long-distance and high-performance driving and can provide shorter optimization times. On the other hand, it was seen that WOA optimization can create vehicle architectures with lower costs, higher maximum speeds, and improved gradability in urban driving. It was found that e-motor 4 and battery 2 can provide the most optimum vehicle architecture solution on a component basis.
(Received in August 2024, accepted in October 2024. This paper was with the authors 1 week for 2 revisions.)

Key Words: Electric Vehicle, Simulink, Design Optimization, Genetic Algorithm, Whale Optimization Algorithm

1. INTRODUCTION

Global population growth is increasing travel and a consequent increase in energy demand [1]. As energy demand increases, energy sources are used more intensively, rapidly increasing environmental pollution. Battery electric vehicles (BEVs) which have reached a high level of importance in recent years, are a technological trend promising to protect environmental health, reduce air pollution, reduce carbon emissions, and leave a cleaner world for future generations.

Studies in the literature [2-4] that include vehicle parameters show that it is appropriate to consider vehicle speed, current, state of charge (SoC), engine speed (RPM), power, torque, energy consumption, range, efficiency, acceleration, and voltage as dynamic variables in vehicle architecture. In daily life, end users usually consider criteria such as dynamic performance, consumption, cost, lifespan, and reliability when choosing a vehicle. Vehicle dynamic performance is a phenomenon that largely depends on the driver's needs. Consumption directly affects the cost of using the vehicle. Users tend to save money by purchasing a vehicle with low consumption. The lifespan of the vehicle may depend on various factors such as durability, maintenance requirements and usage conditions. Vehicles that are less likely to cause problems during use are more likely to be preferred. The reliability of vehicles is very important for users. The absence of unexpected failures and problems is an important feature in terms of reliability. The low risk of failure that may affect long-term use may be a determining factor in terms of reliability when choosing a vehicle. The automotive industry aims to produce vehicles that have adequate performance, low environmental impact, low failure frequency, and provide a satisfactory driving experience by taking into account user expectations.

As in conventional vehicles, the design architecture in electric vehicles also affects vehicle performance [2]. At the heart of the BEV layout is the battery, which optimizes weight

distribution and acts as an energy store, its location and energy capacity affect the vehicle [5]. An on-board charging system is also integrated to charge the battery. The high-efficiency electric motor, which is the core component of the drive system, is placed close to the vehicle's drive axles, which increases efficiency and reduces response time. Unlike conventional vehicles, BEVs do not have to use a traditional multi-gear transmission [6], because the technical specifications of the electric motor allow it to provide sufficient performance over a wide speed range. Since there are no carbon emissions during use, the absence of an exhaust system and tailpipes ensures the simplicity of the BEV layout, making the transportation sector cleaner, more efficient, and more sustainable. It will be easier to achieve the targeted vehicle architecture by optimizing variables such as engine power, battery capacity, and transmission ratio, which directly affect energy consumption and dynamic performance within the subsystems.

Simulation techniques contribute to the ongoing efforts to improve and optimize vehicle performance. As the EV industry continues to evolve, simulations will be invaluable tools that facilitate informed decision-making, increase efficiency, and ensure the longevity of key components, thereby accelerating the transition to a sustainable and technologically advanced future. Simulations offer the advantage of replicating real-world events while saving time and money [7-9]. Various simulation and analysis techniques provide predictions for the systems they represent [10-12]. Simulation techniques designed specifically for BEVs provide valuable information about various evaluation criteria, including energy consumption, performance, and overall lifetime [13, 14]. A detailed simulation system designed for electric vehicles is important in optimizing and improving. By delving into the subcomponents of an electric vehicle, simulation provides detailed information about the operating behaviour of critical elements such as the motor and battery. In battery studies [15], simulations offer significant benefits in predicting the state of charge (SoC) and battery lifetime, which are extremely important parameters in today's dynamic and rapidly changing conditions. They also allow the study of parameters that significantly impact battery lifetime [16].

There are several successful studies in the literature on design optimization of electric vehicles [2, 17-21]. However, there is a gap in the literature on comprehensive optimization methodology of vehicle architecture by considering real driving behaviour. This study develops a design optimization methodology by determining the ideal motor power and battery capacity for a battery electric vehicle according to two different driving profiles. In the study, the virtual vehicle model created in MATLAB/Simulink is subjected to data-driven verification through real driving to save time and cost. The virtual vehicle model created for the optimization process is integrated with GA and WOA. Thanks to the developed methodology, creating an optimal vehicle architecture that is driving-oriented, energy-efficient, and has sufficient dynamic performance is provided.

2. MATERIALS AND METHODS

The optimization study was carried out on the virtual vehicle model created in MATLAB/Simulink, and validated with real data. During the validation process, 6 different parameter data were examined in the CSV file created by CAN-bus record with the VECTOR tool via OBD-II connection during outdoor driving of a real battery electric vehicle. 2 different driving profiles were determined to optimize the vehicle design specifically for driving. In addition, 5 different e-motors and 4 different battery features that are suitable candidates for the vehicle are shared. During the optimization process, the virtual vehicle model was integrated with optimization algorithms, and data flow was provided. The general flow chart of the process can be seen in Fig. 1.

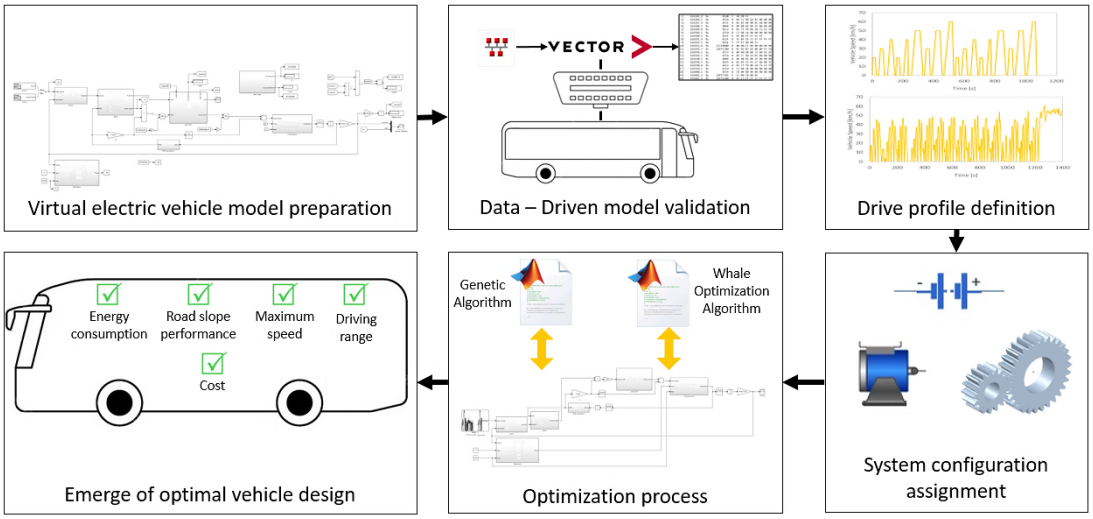

Figure 1: Stages of the study.

2.1 Virtual electric vehicle model

To save time and cost, vehicle architecture optimization was performed on the virtual vehicle model created in MATLAB/Simulink (R2022b). The general view of the virtual vehicle model is in Fig. 2. In the virtual model built on the vehicle dynamic equations, the target speed is subtracted from the actual speed and the torque demand is entered into the driver model. The driver's torque demand and the e-motor speed are processed in the e-motor subsystem to finalize the torque decisions. The battery subsystem controls and provides the requested power, calculating the SoC current and voltage outputs. The battery output power is directed to the transmission system, which converts it into speed by comparing the total resistance forces of the vehicle.

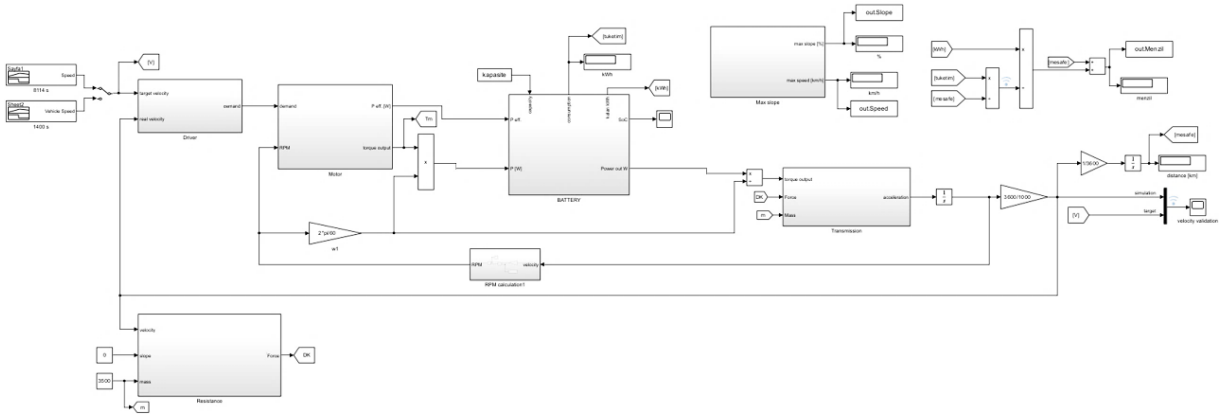

Figure 2: Virtual electric vehicle model illustration.

The driver model determines the torque demand in the vehicle system and transfers it to the motor subsystem for action. For the vehicle model in this study, the velocity difference between the target and the gain is given as input to the driver model.

$$R_{demand} = K_1 \Delta_{velocity} + K_2 \int \Delta_{velocity} + K_3 \frac{d\Delta_{velocity}}{dt} \quad (1)$$

The driver model includes correction parameters such as K_1, K_2, and K_3. Eq. (1) represents the working principle of the driver model. R_{demand} is torque demand that is an output and $\Delta_{velocity}$ is the velocity difference. Correction parameters were set to proper values to accurate output so K_1 is 0.5, K_2 is 0.0001, and K_3 is 0.

Eqs. (2) to (12) expresses the basic dynamics of the traction system in a battery-electric vehicle [9]. Apart from the values specified in the equations, in this study, it is taken into account that the vehicle differential mechanical efficiency is 95 % and the total power consumption of the external components of the traction system is 17 kW.

Eq. (2) expresses the aerodynamic resistance force. This resistance is a resistance that changes depending on the speed of the vehicle. Among the parameters in the equation, ρ is the density of air in kg/m^3, A is the frontal area of the vehicle in m^2, V_v^2 is the vehicle speed in m/s^2, and C_d is the drag coefficient.

$$F_{aero} = \frac{1}{2}\rho A V_v^2 C_d \tag{2}$$

Eq. (3) expresses the rolling resistance force. Rolling resistance coefficient is a variable that depends on speed and tire pressure. Therefore, it is also taken into account in numerical expressions. Eqs. (3) to (5) are for rolling resistance force calculation. In these equations, m is vehicle mass in kg, g is earth gravity in m/s^2, and $\propto$ is road slope in degree. C_{rr} is the rolling resistance coefficient and it includes the static and dynamic stages of the vehicle. The r is the speed correlation. It is hard to define the exact rolling resistance coefficient so there are various approaches to this phenomenon [22]. In this study, the revised version of a rolling resistance coefficient approach was benefited and shared in Eqs. (3) and (4). In Eq. (3), F_{rr} is the rolling resistance force in N. In Eq. (4), Crr_{ref} is the reference value of the rolling resistance coefficient. V is instant speed in km/h. V_{ref} is the reference speed value in km/h. P_{ref} is the reference pressure of the tire in bar. P is the instant pressure of the tire in bar.

$$F_{rr} = mg\ cos(\alpha)\ C_{rr} \tag{3}$$

$$C_{rr} = Crr_{ref} + \left(1 + r\frac{V}{V_{ref}}\right)\left(\frac{P_{ref}}{P}\right) \tag{4}$$

Eq. (5) stands for inertia resistance force. Due to this resistance depends on road slope rate and driving route conditions are highly effective on resistance.

$$F_{gr} = mg\ sin\ (\propto) \tag{5}$$

Eq. (6) is the one of resistance forces that is reasoned by vehicle inertia.

$$F_i = ma \tag{6}$$

Eq. (7) summarizes the total resistance forces that are applied to all vehicles. This force occurs on the diameter of the wheel.

$$F_{resistance} = F_{aero} + F_{rr} + F_{gr} + F_i \tag{7}$$

Eqs. (8) to (10) are wheel torque, motor torque, and motor power which are mechanical behaviour define elements. Parameters that are included in these equations, M_w motor torque in Nm, r_w is wheel radius in m, i_{tr} is transmission ratio, η_{tr} is transmission efficiency, w_m is the angular velocity in rad/s, and P_m is motor power in W.

$$M_w = F_{resistance} * r_w \tag{8}$$

$$M_m = \frac{M_w}{i_{tr}} * \eta_{tr} \tag{9}$$

$$P_m = M_m * w_m \tag{10}$$

The coulomb counting method [23] includes the amount of energy generated per hour of the effect time of the instantaneous power demand and the ratio of the remaining amount of the used amount to the battery capacity. Calculations for charge estimation are given in Eqs. (11) to (12).

$$E_{cons} = \left(\int_0^t P_m \, dt \right) \frac{1}{3600} \tag{11}$$

$$SoC = \left(\frac{E_{battery} - E_{cons}}{V_{nominal}} \right) \frac{1}{3600 \, E_{battery}} 100 \tag{12}$$

In Eqs. (11) and (12), E_{cons} is the consumed energy amount in Wh, $E_{battery}$ is battery full capacity in Wh, and $V_{nominal}$ is battery nominal voltage in V.

The real vehicle used for virtual model validation in the study is a battery-electric minibus. The battery-electric vehicle has a gross vehicle weight of 5000 to 6000 kg and an empty weight of 3000 to 4000 kg. Its length is between 6 and 7 meters, and its front surface area is 5 to 6 square meters. The wheel radius is 0.3 to 0.4 meters, and the aerodynamic drag coefficient is 0.5. The characteristics of the motor and batteries suitable for the vehicle are shared in Tables I and II. All e-motor and battery features are obtained from real off-the-shelf products suitable for the vehicle. Five different e-motor models are Permanent Magnet Synchronous Motor (PMSM) type and their peak power varies between 125 kW and 228 kW. Maximum speeds also vary and according to the features, the highest speed can be reached by e-motor 5.

Table I: e-Motor technical specifications.

	e-Motor 1	**e-Motor 2**	**e-Motor 3**	**e-Motor 4**	**e-Motor 5**
Type	PMSM	PMSM	PMSM	PMSM	PMSM
Maximum power	125 kW	228 kW	130 kW	140–168 kW	150–190 kW
Maximum torque	260 Nm	370 Nm	440 Nm	428 Nm	520 Nm
Maximum speed	11390 rpm	15090 rpm	14000 rpm	16000 rpm	16500 rpm

Table II: Battery technical specifications.

	Battery 1	**Battery 2**	**Battery 3**	**Battery 4**
Type	Lithium-ion	Lithium-ion	Lithium-ion	Lithium-ion
Maximum discharge power	138 kW	112 kW	83 kW	150 kW
Nominal capacity	110 Ah	213 Ah	218 Ah	137 Ah
Nominal energy capacity	42 kWh	80 kWh	62 kWh	52 kWh
Module amount	2	1	2	2

2.2 Virtual vehicle model validation

To evaluate the metrics in a more cost-effective and shorter time in the optimal vehicle architecture creation methodology, the virtual vehicle model in MATLAB/Simulink must be validated. This validation is done through a real-world driving test using data from the CAN bus over an OBD-II connection with the VECTOR vehicle. The real-world driving test lasted 56 seconds on a 0.444 km route with no wind, an ignorable slope, and an outside temperature of 25°C. Since standard driving cycles involve frequent stopping and accelerating, sudden acceleration and regenerative braking were taken into account. Data from the vehicle software system was corrected before the simulation. Fig. 3 shows the speed graph of the real driving test.

2.3 Performance test profiles

To demonstrate the effectiveness of the driving-oriented vehicle design optimization methodology, two driving profiles were considered. The first, “Hybrid Driving”, combines the three types of Standardized Road Test Cycles (SORT) [24] of the Public Transport Association

International: heavy urban, easy urban, and easy suburban [25]. This profile lasts 1072 seconds. The second, “City Driving”, represents real urban driving with frequent stop-and-go conditions and lasts 1400 seconds. The speed profiles of both drivings are shown in Fig. 4.

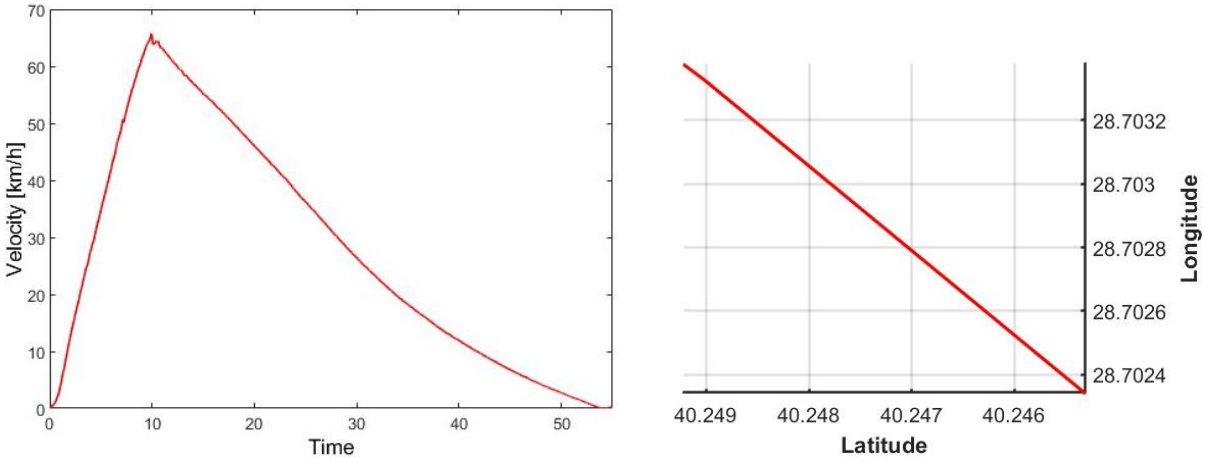

Figure 3: Virtual electric vehicle validation test procedure; vehicle speed (left), test route geographic coordinates (right).

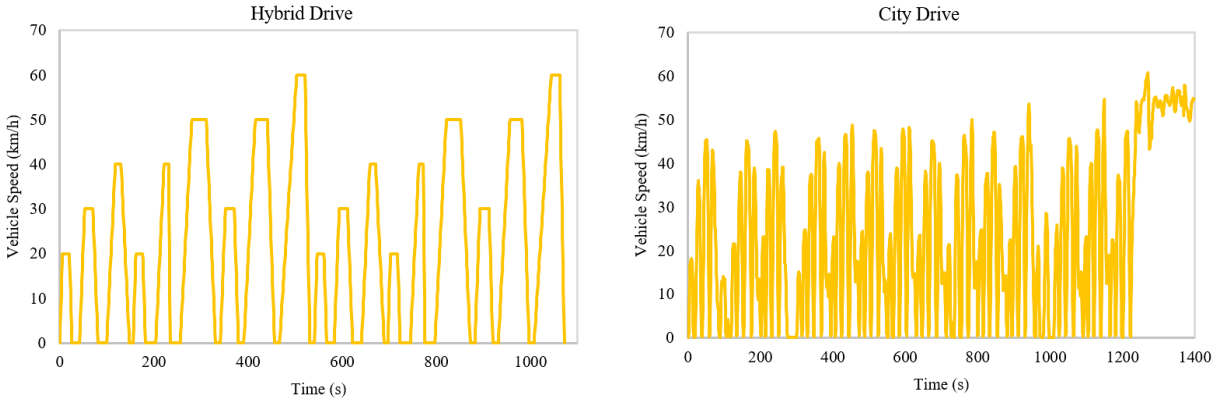

Figure 4: Driving profiles for optimization: hybrid drive (left), city drive (right).

2.4 Design optimization methodology

The battery electric vehicle design optimization methodology is based on the vehicle architecture with a single ratio drive system. The simplified vehicle layout includes a battery for energy storage, an electric motor for converting electrical energy into mechanical energy, and a gearbox for transmission of motion. Recent studies in the literature [26, 27] include advanced model-free, uncertain, multi-dimensional artificial intelligence-based optimal path planning and control policies. The methodology of this study includes GA and WOA methods integrated with MATLAB/Simulink. The algorithms determine the maximum motor power, battery capacity and drive ratio values and share the values with MATLAB Workspace. The virtual vehicle model takes these values as input and runs the system. It provides results such as range, maximum slope capability and maximum speed according to two different driving behaviours. The cost in the fitness function to be minimized is calculated according to the price of motor power and battery capacity determined by the algorithm. The optimization process starts with the highest motor power and battery capacity and finds the optimal solutions at the end of the process. Fig. 5 shows the visual version of the process.

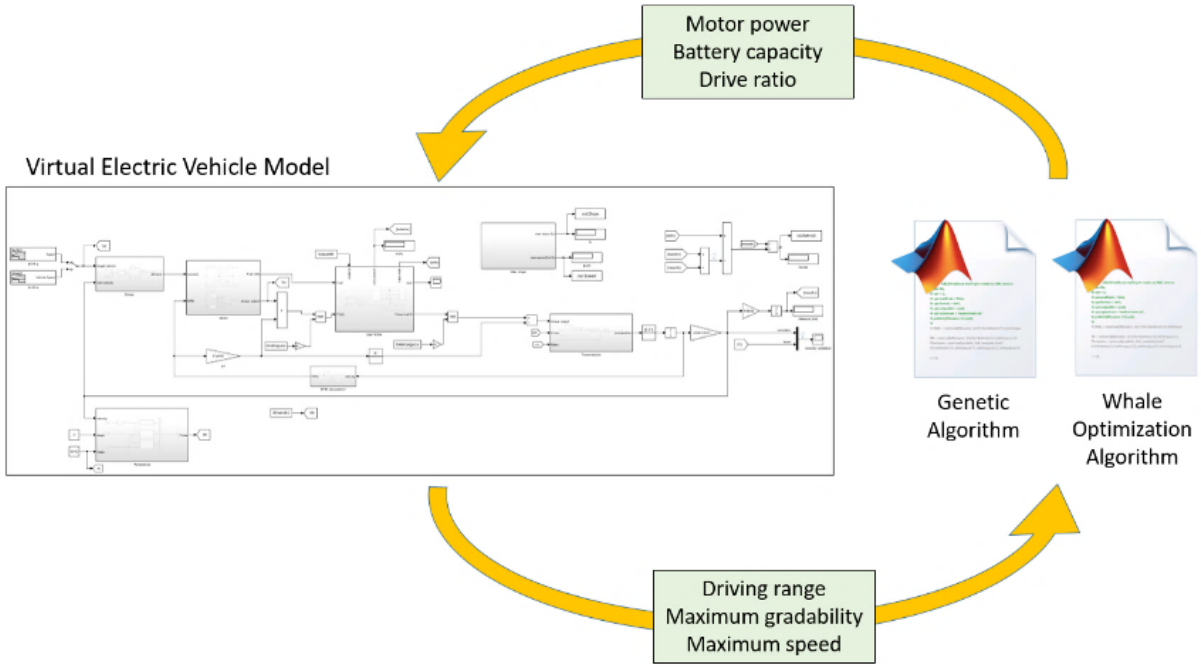

Figure 5: General optimization process flow.

Vehicle architecture optimization methodology aims to minimize the fitness function, which includes parameters such as cost, driving range, maximum gradability, and maximum speed. The input parameters of the optimization process are motor power, battery capacity, and drive ratio value ranges are shared in Eq. (13). In the expressions in Eq. (15) Cost is the total price calculated by multiplying the e-motor power and battery capacity prices determined by the algorithm. At this stage, the price of Lithium-ion battery is considered as 75 $/kWh and the price of PMSM is considered as 3.3 $/kW [28, 29]. The fitness function prepared for the optimization process is given in Eq. (14). The calculation of the estimated cost value is given in Eq. (15). The range, slope, and speed values are direct outputs of the Simulink model. The range is the driving distance that the vehicle can reach in the specified configuration according to the iteration and mostly varies between 140 km and 240 km. The slope is the maximum road slope that the vehicle can reach in the specified architecture, between 15 % and 40 % in the study. The speed is the maximum speed that the vehicle configuration can reach on a flat road, between 100 km/h and 112 km/h. The combination of these parameters and the lowest Fitness function result was selected as the most optimal vehicle architecture for driving behaviour.

$$\begin{gathered} 125 < \text{motor power} < 228 \\ 80 < \text{battery capacity} < 124 \\ 18.4 < \text{drive ratio} < 32 \end{gathered} \tag{13}$$

$$\text{Fitness} = \text{Cost} - \text{Range} - \text{Slope} - \text{Speed} \tag{14}$$

$$\text{Cost} = 3.3 \cdot \text{motor power} + 75 \cdot \text{battery capacity} \tag{15}$$

The GA is a computational method used to solve complex optimization problems by simulating the flow in the natural evolution process. Inspired by the basic principles of biological evolution, it tries to find the most appropriate solutions in the solution space. Its basic functions include biological concepts such as population, chromosome, fitness function, selection, cross-over, and mutation. In a GA, the solution process starts with a population. Each individual (chromosome) within the population represents a potential solution. The chromosome consists of smaller units called genes and is the encoded version of the parameters that define the problem. The fitness function is an evaluation criterion that shows how well individuals do in a targeted condition. It is defined specifically for the optimization problem

and is generally a function that searches for the maximum or minimum value. Selection ensures that individuals with high fitness values in the population are transferred to the next generation. Roulette wheel selection and tournament selection are frequently used selection methods. Crossover is the creation of new individuals by combining two chromosomes. Genetic diversity is increased, allowing better solutions to be found. The mutation increases genetic diversity through small changes in the genes of chromosomes, and the mutation rate is generally kept low [30, 31].

The WOA is a nature-inspired metaheuristic optimization algorithm [32]. Optimization methodology in WOA is similar to other nature-inspired algorithms such as the bald eagle search algorithm [33]. WOA mimics the hunting behaviour of humpback whales. Humpback whales can sense the location of their prey and surround them. Since the position of the optimal solution in the search volume is not known in advance, WOA considers the current best candidate solution to be close to optimal. Once the best search agent is identified, other search agents try to update their positions to the best search agent. In WOA, the lead whale finds prey and dives down, creating a spiral set of bubbles around the prey and trapping them in a bubble network. It then swims towards the surface, following the bubbles. Other whales behind the leader form a formation and take the same position with each move. Fig. 6 shows the GA and WOA optimization flows.

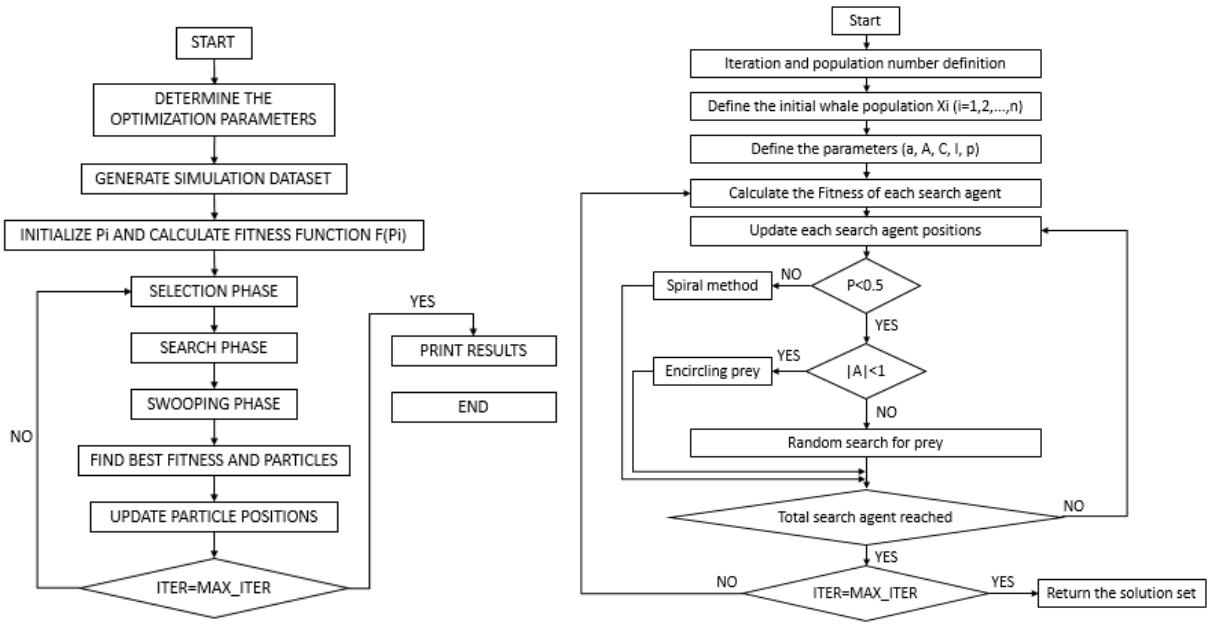

Figure 6: Optimization process with GA flow (left) and WOA flow (right).

3. RESULTS

In the study targeting the optimal vehicle architecture creation methodology, metaheuristic optimization methods were used. The developed methodology is capable of providing outputs that will illuminate the start and process of driving-optimal vehicle design. The study was carried out on a verified virtual vehicle model for cost and time-saving purposes. The results obtained in the virtual vehicle verification were compared with the real data in the study. In addition, the effective force values obtained in the virtual model verification test were shared. The verified virtual model interacted with the methods used in the development of the optimization methodology.

3.1 Virtual electric vehicle model validation results

A real-world driving test was carried out to ensure the accuracy of the virtual electric vehicle model. The performance result graphs by real and virtual models were laminated to see the difference. Although local deviations were observed in the result values due to parameter assumptions made for the virtual model and unevenness of the real road. The velocity, motor torque, and motor power results showed that the virtual model validation was adequately achieved. Under this driving condition, the real electric vehicle consumed 0.1154 kWh of energy, while the virtual vehicle model consumed 0.1145 kWh. According to this result, a deviation of 0.7 % occurred. Result comparison graphs are shared in Fig. 7.

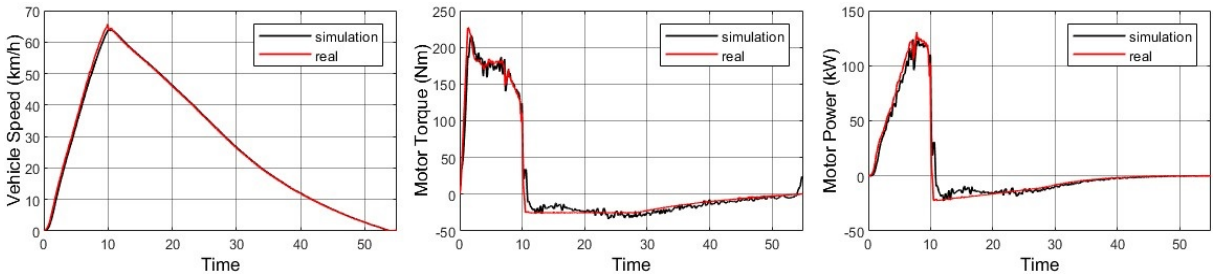

a) b) c)

Figure 7: BEV model validation graphs: a) velocity, b) motor torque, c) motor power.

Since the vehicle was used with sudden acceleration demand, there was a sudden increase, especially in torque and power graphics. During the deceleration phase, some of the energy lost during acceleration was recovered with the help of regenerative braking.

3.2 Design optimization methodology results

The optimization methodology began with the highest motor power and battery capacity. Initially, the vehicle featured a 228 kW motor, reaching a maximum speed of 112 km/h, and a 124 kWh battery providing a 105.4 km range per charge. The 18.4 drive ratio effectively transmitted motor power to the wheels. The vehicle could climb a 35 % slope, have an efficiency of 1.08 kWh/km, and cost $10085.

Tables III, IV, and V show optimal results for unloaded, half-loaded, and fully-loaded driving cycles. These tables include maximum speed, slope capability, and driving range values for motor power, battery capacity, and drive ratio. They also provide energy efficiency (battery capacity/driving range), cost, and optimization algorithm runtime.

Table III: Optimal solutions for unloaded vehicle.

	Hybrid drive		**City drive**	
	GA optimized	**WOA optimized**	**GA optimized**	**WOA optimized**
e-Motor power	137.34 kW	138.19 kW	138.74 kW	135.02 kW
Battery capacity	80.55 kWh	80.21 kWh	79.17 kWh	79 kWh
Driving range	233.84 km	229.34 km	148.87 km	140.34 km
Drive ratio	19.15	18.64	20.22	18.43
Maximum speed	108.20 km/h	111.17 km/h	102.49 km/h	112.42 km/h
Maximum grade	34.31 %	32.39 %	41.24 %	40.02 %
Efficiency	0.34 kWh/km	0.35 kWh/km	0.53 kWh/km	0.56 kWh/km
Cost	US$ 6494.62	US$ 6472.09	US$ 6395.65	US$ 6370.59
Elapsed time	1148.54 s	1418.57 s	2034.98 s	2146.35 s

Table IV: Optimal solutions for half-loaded vehicle.

	Hybrid drive		City drive	
	GA optimized	**WOA optimized**	**GA optimized**	**WOA optimized**
e-Motor power	139.05 kW	137.16 kW	140.40 kW	136.71 kW
Battery capacity	79.49 kWh	80.55 kWh	81.37 kWh	79 kWh
Driving range	199.74 km	201.92 km	110.91 km	107.17 km
Drive ratio	18.58	18.73	18.77	18.49
Maximum speed	111.51 km/h	110.60 km/h	110.37 km/h	112.05 km/h
Maximum grade	22.56 %	25.76 %	36.03 %	40.27 %
Efficiency	0.39 kWh/km	0.40 kWh/km	0.73 kWh/km	0.74 kWh/km
Cost	US$ 6420.79	US$ 6493.89	US$ 6566.18	US$ 6376.13
Elapsed time	1260.98 s	1361.70 s	1914.64 s	1987.76 s

Table V: Optimal solutions for fully-loaded vehicle.

	Hybrid drive		City drive	
	GA optimized	**WOA optimized**	**GA optimized**	**WOA optimized**
e-Motor power	142.56 kW	142.99 kW	138.52 kW	135.10 kW
Battery capacity	79.38 kWh	79 kWh	83.27 kWh	79.25 kWh
Driving range	164.09 km	162.73 km	91.13 km	85.51 km
Drive ratio	18.74	18.44	18.89	18.50
Maximum speed	110.55 km/h	112.35 km/h	109.68 km/h	112.60 km/h
Maximum grade	17.69 %	21.56 %	37.27 %	38.75 %
Efficiency	0.48 kWh/km	0.49 kWh/km	0.91 kWh/km	0.93 kWh/km
Cost	US$ 6423.69	US$ 6396.86	US$ 6702.80	US$ 6370.51
Elapsed time	1176.82 s	1296.69 s	1835.94 s	1943.15 s

4. CONCLUSION

Determining driver expectations is critical to developing an optimized vehicle architecture. Prioritizing factors such as energy efficiency, cost, and performance helps select the most appropriate optimization method for vehicle design. When carefully considering these factors throughout the design and optimization process, the vehicle is more likely to achieve operational efficiency and cost-effectiveness. Using the right optimization strategy, it is possible to create solutions that effectively balance energy efficiency, cost, and performance, leading to a vehicle design that meets technical requirements and user expectations. In this study, a vehicle design optimization methodology was developed for two different real-world driving conditions and three different vehicle mass configurations. These configurations were compared in terms of performance, cost, and efficiency. The results show that different optimization algorithms yield different results depending on the intended use of the vehicle. In particular, Genetic Algorithm (GA) optimization is more effective for long-distance, high-performance driving, where efficiency and speed are critical. In contrast, the Whale Optimization Algorithm (WOA) produced vehicle designs that are more suitable for urban driving, where cost-effectiveness, maximum speed, and gradability are more important. Furthermore, the analysis found that e-motor 4 consistently delivered optimum motor power across all driving profiles and mass configurations, while battery 2 was the most suitable option to meet battery requirements. The study highlights how optimization methodologies can address specific vehicle needs, such as power output for long-distance driving or cost-effectiveness for urban environments. Future research could include testing additional driving conditions and exploring different optimization algorithms to improve design accuracy. Incorporating lifecycle assessments could address the environmental impacts of vehicle designs. An interdisciplinary approach that combines electrical component optimization with

detailed battery management strategies will further improve energy management in future vehicle models.

ACKNOWLEDGEMENT

The authors are presenting their appreciation to TUBITAK (project code 119C154) the support in the preparation of this study.

REFERENCES

[1] Yavaş, Ö.; Savran, E.; Nalbur, B. E.; Karpat, F. (2022). Energy and carbon loss management in an electric bus factory for energy sustainability, *Transdisciplinary Journal of Engineering & Science*, Vol. 13, SP-2, 97-110, doi:10.22545/2022/00207

[2] Tran, M.-K.; Akinsanya, M.; Panchal, S.; Fraser, R.; Fowler, M. (2021). Design of a hybrid electric vehicle powertrain for performance optimization considering various powertrain components and configurations, *Vehicles*, Vol. 3, No. 1, 20-32, doi:10.3390/vehicles3010002

[3] Sharmila, B.; Srinivasan, K.; Devasena, D.; Suresh, M.; Panchal, H.; Ashokkumar, R.; Meenakumari, R.; Sadasivuni, K. K.; Shah, R. R. (2021). Modelling and performance analysis of electric vehicle, *International Journal of Ambient Energy*, Vol. 43, No. 1, 5034-5040, doi:10.1080/01430750.2021.1932587

[4] Rosas-Cervantes, D.; Fernández-Ramos, J. (2023). Simulation tool for assessing driving strategies for electric racing vehicles, *World Electric Vehicle Journal*, Vol. 14, No. 8, Paper 198, 23 pages, doi:10.3390/wevj14080198

[5] Özdemir, M.; Erdoğan, E. O. (2023). Determination of optimal battery locations for ride comfort in electric automobiles using a nonlinear half-vehicle suspension model, *Journal of the Faculty of Engineering and Architecture of Gazi University*, Vol. 39, No. 1, 339-350, doi:10.17341/gazimmfd.1181623

[6] Ntombela, M.; Musasa, K.; Moloi, K. (2023). A comprehensive review for battery electric vehicles (BEV) drive circuits technology, operations, and challenges, *World Electric Vehicle Journal*, Vol. 14, No. 7, Paper 195, 23 pages, doi:10.3390/wevj14070195

[7] Rodrigues, M. V. T.; Sirova, E.; Dyntar, J. (2022). Maintenance scheduling of heating networks using simulation in Witness, *International Journal of Simulation Modelling*, Vol. 21, No. 2, 203-213, doi:10.2507/IJSIMM21-2-590

[8] Straka, M. (2023). Design of microgrids as a cost economy energy savings simulation model: Monte Carlo method, *International Journal of Simulation Modelling*, Vol. 22, No. 4, 586-597, doi:10.2507/IJSIMM22-4-659

[9] Savran, E.; Karpat, E.; Karpat, F. (2024). Fuel cell electric vehicle hydrogen consumption and battery cycle optimization using bald eagle search algorithm, *Applied Sciences*, Vol. 14, No. 17, Paper 7744, 19 pages, doi:10.3390/app14177744

[10] Turan, M. K.; Ensarioglu, C.; Bakirci, A.; Karpat, F. (2024). Impact performance of unconventional trigger holes, *Materials Testing*, Vol. 66, No. 3, 389-396, doi:10.1515/mt-2023-0253

[11] Savran, E.; Karpat, E.; Karpat, F. (2024). Energy-efficient anomaly detection and chaoticity in electric, *Sensors*, Vol. 24, No. 17, Paper 5628, 27 pages, doi:10.3390/s24175628

[12] Savran, E.; Karpat, F. (2024). Synthetic data generation using Copula model and driving behavior analysis, *Ain Shams Engineering Journal*, Paper 103060, 6 pages, in press, doi:10.1016/j.asej.2024.103060

[13] Bin Ahmad, M. S.; Pesyridis, A.; Sphicas, P.; Mahmoudzadeh Andwari, A.; Gharehghani, A.; Vaglieco, B. M. (2022). Electric vehicle modelling for future technology and market penetration analysis, *Frontiers in Mechanical Engineering*, Vol. 8, Paper 896547, 18 pages, doi:10.3389/fmech.2022.896547

[14] Sun, J.; Liu, S. F.; Zhang, X. H.; Gong, D. Q. (2022). Simulation-based modelling of the impact of ridesharing on urban system, *International Journal of Simulation Modelling*, Vol. 21, No. 1, 148-159, doi:10.2507/IJSIMM21-1-CO2

[15] Qin, D.; Li, J.; Wang, T.; Zhang, D. (2019). Modeling and simulating a battery for an electric vehicle based on Modelica, *Automotive Innovation*, Vol. 2, No. 3, 169-177, doi:10.1007/s42154-019-00066-0
[16] Wang, T.; Zhang, X.; Zeng, Q. L.; Jiang, S. B.; Zhang, Y. N. (2022). Modelling and simulation on cavity cold plate for Li-ion battery thermal management, *International Journal of Simulation Modelling*, Vol. 21, No. 1, 65-76, doi:10.2507/IJSIMM21-1-588
[17] Kwon, K.; Seo, M.; Min, S. (2020). Multi-objective optimization of powertrain components for electric vehicles using a two-stage analysis model, *International Journal of Automotive Technology*, Vol. 21, No. 6, 1495-1505, doi:10.1007/s12239-020-0141-5
[18] Schumacher, S.; Schmid, S.; Wieser, P.; Stetter, R.; Till, M. (2021). Design, simulation and optimization of an electrical drive-train, *Vehicles*, Vol. 3, No. 3, 390-405, doi:10.3390/vehicles3030024
[19] Othaganont, P.; Assadian, F.; Auger, D. J. (2017). Multi-objective optimisation for battery electric vehicle powertrain topologies, *Proceedings of the Institution of Mechanical Engineers, Part D: Journal of Automobile Engineering*, Vol. 231, No. 8, 1046-1065, doi:10.1177/0954407016671275
[20] Verbruggen, F. J. R.; Silvas, E.; Hofman, T. (2020). Electric powertrain topology analysis and design for heavy-duty trucks, *Energies*, Vol. 13, No. 10, Paper 2434, 30 pages, doi:10.3390/en13102434
[21] Hu, J.; Cao, W.; Jiang, F.; Hu, L.; Chen, Q.; Zheng, W.; Zhou, J. (2023). Study on multi-objective optimization of power system parameters of battery electric vehicles, *Sustainability*, Vol. 15, No. 10, Paper 8219, 23 pages, doi:10.3390/su15108219
[22] Song, J.; Cha, J. (2021). Analysis of driving dynamics considering driving resistances in on-road driving, *Energies*, Vol. 14, No. 12, Paper 3408, 16 pages, doi:10.3390/en14123408
[23] Movassagh, K.; Raihan, A.; Balasingam, B.; Pattipati, K. (2021). A critical look at Coulomb counting approach for state of charge estimation in batteries, *Energies*, Vol. 14, No. 14, Paper 4074, 33 pages, doi:10.3390/en14144074
[24] The International Association of Public Transport. Advancing Public Transport, from *https://www.uitp.org/*, accessed on 12-09-2024
[25] The International Association of Public Transport. UITP SORT & E-SORT Brochures, from *https://www.uitp.org/publications/uitp-sort-e-sort-brochures/*, accessed on 12-09-2024
[26] Tutsoy, O.; Asadi, D.; Ahmadi, K.; Nabavi-Chashmi, S. Y.; Iqbal, J. (2024). Minimum distance and minimum time optimal path planning with bioinspired machine learning algorithms for faulty unmanned air vehicles, *IEEE Transactions on Intelligent Transportation Systems*, Vol. 25, No. 8, 9069-9077, doi:10.1109/TITS.2024.3367769
[27] Riaz, S.; Qi, R.; Tutsoy, O.; Iqbal, J. (2023). A novel adaptive PD-type iterative learning control of the PMSM servo system with the friction uncertainty in low speeds, *PLoS ONE*, Vol. 18, No. 1, Paper e0279253, 22 pages, doi:10.1371/journal.pone.0279253
[28] Orangi, S.; Manjong, N.; Clos, D. P.; Usai, L.; Burheim, O. S.; Strømman, A. H. (2024). Historical and prospective lithium-ion battery cost trajectories from a bottom-up production modeling perspective, *Journal of Energy Storage*, Vol. 76, Paper 109800, 14 pages, doi:10.1016/j.est.2023.109800
[29] Cai, W.; Wu, X.; Zhou, M.; Liang, Y.; Wang, Y. (2021). Review and development of electric motor systems and electric powertrains for new energy vehicles, *Automotive Innovation*, Vol. 4, No. 1, 3-22, doi:10.1007/s42154-021-00139-z
[30] Aivaliotis-Apostolopoulos, P.; Loukidis, D. (2022). Swarming genetic algorithm: a nested fully coupled hybrid of genetic algorithm and particle swarm optimization, *PLoS ONE*, Vol. 17, No. 9, Paper e0275094, 24 pages, doi:10.1371/journal.pone.0275094
[31] Yang, D.; Yu, Z.; Yuan, H.; Cui, Y. (2022). An improved genetic algorithm and its application in neural network adversarial attack, *PLoS ONE*, Vol. 17, No. 5, Paper e0267970, 17 pages, doi:10.1371/journal.pone.0267970
[32] Mirjalili, S.; Lewis, A. (2016). The whale optimization algorithm, *Advances in Engineering Software*, Vol. 95, 51-67, doi:10.1016/j.advengsoft.2016.01.008
[33] Kankılıç, S.; Karpat, E. (2023). Optimization of multilayer absorbers using the bald eagle optimization algorithm, *Applied Sciences*, Vol. 13, No. 18, Paper 10301, 17 pages, doi:10.3390/app131810301